Detection of Changes in Lateral Weight Shift During Gait Improvement of Patients via Image Analysis of Frontal-Direction Imaging Using MediaPipe

Yasutaka Uchida
Dept. of Life Science,
Teikyo University of Science
Tokyo, Japan
e-mail: uchida@ntu.ac.jp

Eiichi Ohkubo
Dept. of Life Science,
Teikyo University of Science
Tokyo, Japan
e-mail: ohkubo@ntu.ac.jp

Yasunori Fujimori
Dept. of Rehabilitation
Seirei Yokohama Hospital
Yokohama, Japan
e-mail: yasu6622@outlook.jp

Tomoko Funayama
Dept. of Occupational Therapy
Teikyo University of Science
Yamanashi, Japan
e-mail: funayama@ntu.ac.jp

Daisuke Souma
Dept. of Rehabilitation
Isogo Central Hospital
Yokohama, Japan
e-mail: rifles060920@gmail.com

Yoshiaki Kogure
Professor Emeritus
Teikyo University of Science
Tokyo, Japan
e-mail: kogure@ntu.ac.jp

***Abstract*—Obtaining numerical skeletal data is important for objectively assessing a patient's gait status. Using MediaPipe on images captured from the frontal plane—a method not limited by the imaging-facility size—we use skeletal data to evaluate walking changes caused by the rehabilitation of three patients over a period of approximately one month. To reduce errors due to differences in participant picture size, two methods are examined: one based on waist width and the other on shoulder width. Using standardized data, we examine the changes in the nose position, left and right ankle heights, and left and right shoulder slopes, as well as the differences between toes and heels, and between the left and right elbow widths. Additionally, the appearance of each part of the body during walking is examined via spectrograms. Despite the few participants, the findings suggest that not only the stride length and foot speed but also the blurring of the nose position, left and right elbow positions, and ankle and knee can be used as indicators to assess whether weight is being shifted smoothly during walking as well as to evaluate the degree of recovery from rehabilitation.**

Keywords—MediaPipe; rehabilitation evaluation; digital health; frontal-direction image; gait analysis; lateral weight shift.

I. INTRODUCTION

Assessing changes in a patient's condition is crucial for rehabilitation [1]-[4]. Gait assessments in clinical settings reveal considerable potential health status and predictive information. Quantitative instrumented gait analysis is recommended for clinical gait assessment; however, its use is currently limited. Owing to recent advances in machine-learning research, studies pertaining to rehabilitation recovery are increasing rapidly. According to previous studies, various sensors are used to measure the time required to perform a defined exercise, and the data are used in machine-learning methods such as k-nearest neighbor approximation, support vector machine, random forest, and logistic regression [5].

Spatiotemporal parameters during gait are considered effective for quantifying gait performance and determining the state of physical functions. Measurement units are not limited by the measurement space as they do not require a pre-installed three-dimensional motion-capture system, for instance the system released by Vicon Motion Systems Ltd. UK, which is used as the de facto standard; however, this standard must be validated [6][7].

Kinect for Windows v1, which is released by Microsoft, features a red-green-blue camera for color videos and an infrared (IR) emitter. The camera allows depth measurement when the baseline between the camera and projector is known. Meanwhile, Kinect for Windows v2 offers improved skeleton tracking. Azure Kinect DK, which was released in 2019, integrates artificial-intelligence applications. The potential for realizing clinical applications using the Azure Kinect camera, which is continuously being improved, is currently being investigated [8]-[12].

Recent advances in machine learning and other technologies have enabled skeletal recognition in software such as OpenPose [13]-[17] without using IR cameras such as the Kinect. OpenPose is currently used for knee- and ankle-motion analyses because it can estimate whole-body skeletons and human postures. MediaPipe [18]-[29] supports various frameworks and uses video cameras and images captured by smartphone cameras for analysis. It offers advantages such as the use of a high-performance graphics processing units through Google Colaboratory. However, no-code programming is currently possible, although it requires understanding regarding the source code. Therefore, applications such as reporting gait analysis are rare. Additionally, because the rehabilitation area is required for video recording, analysis from the sagittal-plane direction is challenging, and only a few implementation cases have been reported.

At a conference held last year, we reported the possibility of using MediaPipe to analyze images captured from the frontal plane based on the stride length and ankle angle. Additionally, we measured the gait of participants who underwent physical and occupational therapy training and verified the effectiveness of walking aids in participants who required hospitalization. The effectiveness of the walking aids was verified as follows: the dispersion of the nose position in the left and right directions was used as an index of body shaking during walking; the tilt of the shoulders, hips, and neck during walking was calculated using MediaPipe data to determine balance; and the time variation of these data was used as the basis for discrete Fourier spectrum decomposition and heel spectrograms. The effect of the walking aids on the participants' gait was demonstrated from multiple perspectives.

In this study, we use a method reported in the literature for participants under different conditions; subsequently, we examine the differences and attempt to improve the accuracy. The remainder of this paper is organized as follows: Section II presents the experimental conditions. In Section III, we present the experimental results obtained via characteristic observations performed by participants undergoing rehabilitation, as previously reported, toward other participants and analyze them from a new perspective. Section IV discusses the obtained results. The proposed method reduces the effect of the distance from the camera through hip or shoulder-width standardization. Changes in gait are confirmed by determining the nose position, height at the feet, tilt of the right and left shoulders, toe and heel widths, and elbow width during gait, as well as based on spectrograms. Section V concludes the paper.

This study was approved by the Ethics Committee on Research with Humans as Participants of the Teikyo University of Science. The participants received written informed consent from the physical therapist at the hospital where they were admitted.

II. EXPERIMENTS

Video recordings of walking conditions on the ORPHE ANALYTICS screen were captured using a snipping tool and analyzed using MediaPipe. During the measurements, walking at a distance of 3 m from the front was recorded using a smartphone camera. Participant A was a female in her 40s. She was diagnosed with right capsular hemorrhage, and her disabilities included left hemiplegia and severe sensory impairment. Prior to the onset of stroke, she was able to perform daily activities independently, was employed full-time five days a week, and commuted to work using public transportation. She was transferred to the hospital for convalescent rehabilitation approximately two weeks after the onset of stroke. Physical therapy (120 min) and occupational therapy (60 min) were provided to the patient, and gait training was conducted during physical therapy. The first image was captured 72 d after stroke onset, and the second image was captured on the 109th day. The patient was discharged from the hospital 4 d after the video recording, and rehabilitation was performed on an outpatient basis (Participant A). When she was discharged from the hospital, she walked outdoors with the assistance of a T-cane and short leg brace.

Participant B was a right-handed man in his 70s. He was diagnosed with left atherothrombotic cerebral infarction, right hemiplegia, and mild deep sensory dullness. His medical history included a cervical spinal-cord injury (difficulty in lifting the right upper limb), lung-cancer surgery, and pharyngeal cancer (currently undergoing radiation therapy). Prior to the onset of cerebral infarction, his daily activities included crawling indoors. He was transferred to Isog Central Hospital 18 d after the onset of stroke for rehabilitation and was underwent 60–80 minutes of physical therapy and 60 min of occupational therapy seven times a week, during which he underwent walking training.

Participant C was a right-handed man in his 60s. He was diagnosed with left thalamic hemorrhage and right hemiplegia, and anesthesia. His medical history included chronic heart failure, hypertension, chronic kidney disease, schizophrenia, colonic polyps, and gastroesophageal reflux disease. Before the onset of cerebral hemorrhage, the patient lived alone and was able to perform daily activities independently, including outdoor activities. He was transferred to Isogo Central Hospital on the day of the onset for blood-pressure management and follow-up. Subsequently, 29 days after the onset, he was transferred to our hospital's rehabilitation ward for continued rehabilitation, where he received 120 min of physical therapy and 60 min of occupational therapy seven times a week, including gait training.

For reference, a participant without walking disabilities (Participant D in this study) videotaped a male participant in his 60s at Teikyo University of Science. The video of Participant D's analysis was captured using a camera.

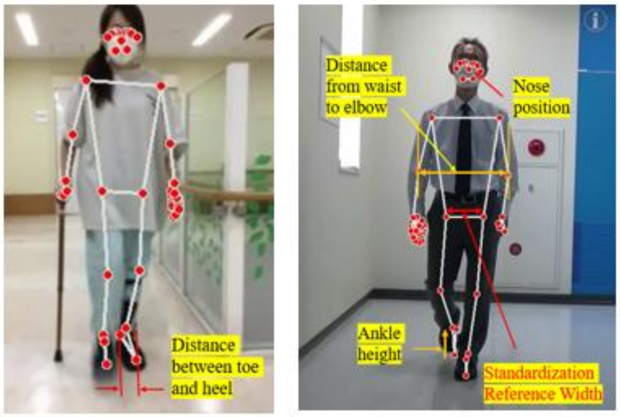

(a) Participant A (b) Participant D

Figure 1. Definition of evaluation parameters.

As shown in Figure 1, the waist width was used as the standard, and the coordinates of each part were assigned and normalized using this value. This was performed to address measurement errors in parameters during walking, such as the stride length, caused by the small image of the participant at the start of walking. Additionally, it enabled one to determine the stride length and foot speed more easily based on the measurement results. The values shown in the results were defined as the distance between the toes and heel, the nose position, the distance from the waist to the elbow, and the ankle height, as shown in Figures 1(a) and 1(b).

We used a wireless smart insole (FEELSOLE®) equipped with pressure sensors, which enabled four parts (the toe, heel, inside, and outside) of each foot to be measured, thus resulting in eight parts for both feet. The insoles were calibrated before use. Calibration was performed four times: with no pressure or feet in shoes, standing on both feet, and standing on one foot on each side. The sampling frequency was set to 50 Hz. Data were stored on the cloud using ORPHE ANALYTICS and downloaded in the CSV format [30].

III. Experimental Results

A. *Height of left and right ankles*

When the images were captured from the front, owing to the features of MediaPipe, the z-axis values increased as the participant approached the camera. The z-axis values of the ankles and other parts of the body at the start of walking were normalized by the width of the hips to avoid ambiguity in the gait conditions, such as the stride length. Figure 2 shows the left and right ankle heights normalized by the hip width for the participant 72 d after onset. Figure 3 shows the ankle height of the same participant 109 d after the onset, normalized by the hip width. In Figures 2 and 3, the horizontal axis shows the time in seconds, and the vertical axis shows the ankle position from the normalized waist.

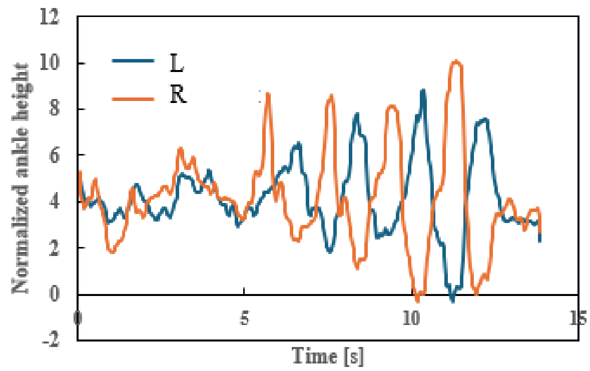

Figure 2. Normalized ankle height during gait 72 d after onset.

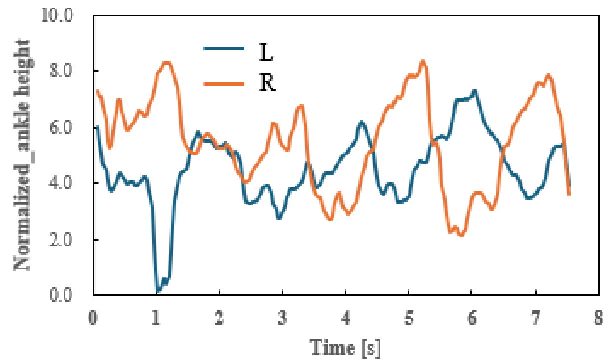

Figure 3. Normalized ankle height during gait measured 109 d after onset.

B. *Normalized shoulder angle*

The results at the beginning of rehabilitation and after five weeks are presented in Figures 4 and 5, respectively. They were obtained from the inner product of vectors using the coordinates of the left shoulder as the origin and the right shoulder angle with respect to the horizontal direction, normalized by the hip width. Difference in blurring was observed at the beginning of walking between the measurements obtained 72 and 109 d after the onset.

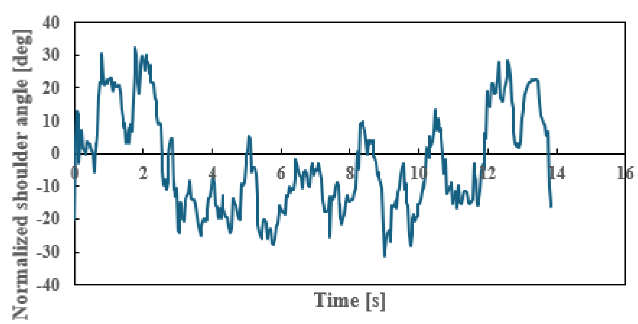

Figure 4. Angle of right shoulder with respect to left shoulder 72 d after onset.

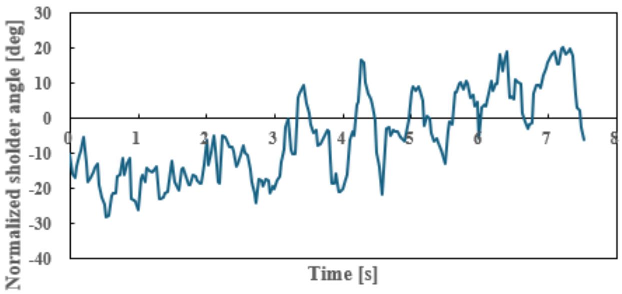

Figure 5. Angle of right shoulder with respect to left shoulder 109 d after onset.

In Figures 4 and 5, the horizontal axis represents time in seconds, and the vertical axis represents the normalized shoulder angle in degrees.

C. *Blurring of nose position*

We observed that the camera position was slightly off the frontal direction in the direction of gait owing to restrictions at the rehabilitation site during filming. Hence, a normalized nose center position was obtained as a linear function, and the difference from the center position was defined as the nose shake.

Figures 6 and 7 show the lateral swing of Participant A's nose during walking, as observed from the frontal direction at 72 and 109 d after onset, respectively. The initial measurement at 72 d after the onset showed minor blurring at the beginning of walking because the participant required more time to begin walking, as compared with the measurement at 109 d after the onset. However, the overall variation in amplitude was approximately similar when viewed over the entire time period. The red and green circles indicate misalignments to the left and right sides of the body, respectively. In Figures 6–11, nose blurring is shown as time on the horizontal axis in seconds, and normalized nose position blurring variance is shown on the vertical axis.

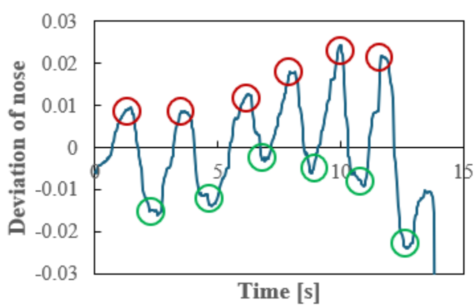

Figure 6. Nasal blurring in left and right directions 72 d after onset.

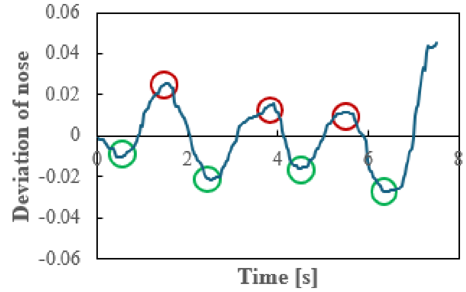

Figure 7. Nasal blurring in left and right directions 109 d after onset.

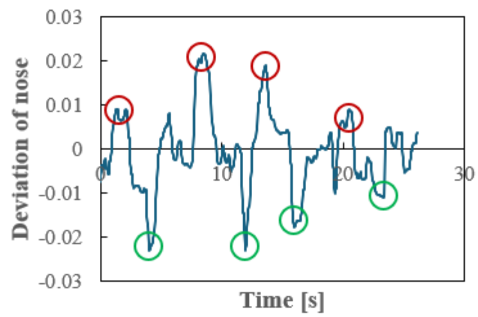

Figure 8. Nasal blurring in left and right directions 46 d after onset.

Figures 8 and 9 show the lateral swing of Participant B's nose during walking, as observed from the frontal direction at 46 and 79 days after onset, respectively.

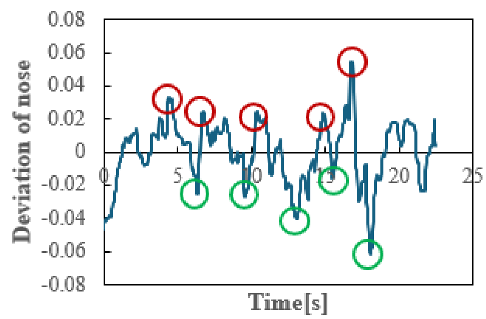

Figure 9. Nasal blurring in left and right directions 79 d after symptom onset.

Regarding the blurring of the nose, the camera was set almost in front of the participant; however, the participant shifted from the center of the screen while walking toward the camera. Figures 6–11 show the first and second measurement results for Participants A, B, and C after calculating the deviation from the approximate straight line and performing corrections, respectively. The red and blue circles in the figure represent the peak of the participant's nasal blurring to the left and right, respectively.

Figures 10 and 11 show the lateral swing of Participant C's nose during walking, as observed in the frontal plane at 44 and 72 d after onset, respectively.

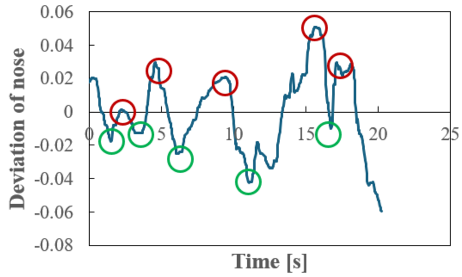

Figure 10. Nasal blurring in left and right directions 44 d after onset.

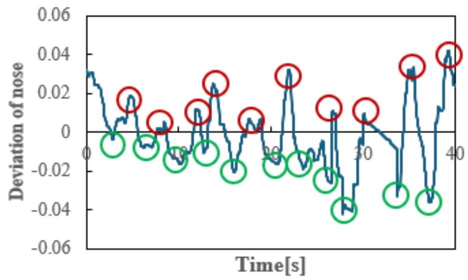

Figure 11. Nasal blurring in left and right directions 72 d after onset.

Table 1. Standard deviation of nasal blurring for each participant.

	1st measurement	2nd measurement
A	1.03E-2	1.65E-2
B	8.74E-3	1.90E-2
C	2.37E-2	1.72E-2

By adopting a methodology reported in the literature, the standard deviation of nasal blurring for each participant during the first and second measurements is as shown in Table 1.

Table 2 shows the average values of the leftward and rightward nasal swings as well as the difference between them for the participants, as indicated by red circles in the graph of the first measurement results.

Table 3 shows the average values of the leftward and rightward nasal swings as well as the difference between them for the participants indicated by red circles in the graph of the second measurement results.

Table 2. Left and right shift results of first measurement.

	Left shift	Right shift	L-R
A	0.0159	-0.0121	0.028
B	0.0109	-0.0188	0.030
C	0.0264	-0.0216	0.048

Table 3. Left and right shift results of second measurement.

	Left shift	Right shift	L-R
A	0.0178	-0.0188	0.037
B	0.0319	-0.034	0.066
C	0.0197	-0.0214	0.041

D. *Change in width between toe and heel*

Figures 12 and 13 show the changes in the width between the toes and heel of the left and right feet at 72 and 109 days after onset, respectively. As depicted, the width was smaller at 109 d after the onset. The horizontal axes in Figures 12 and 13 show the time in seconds, and the vertical axes show the normalized left and right toe widths normalized by the waist width.

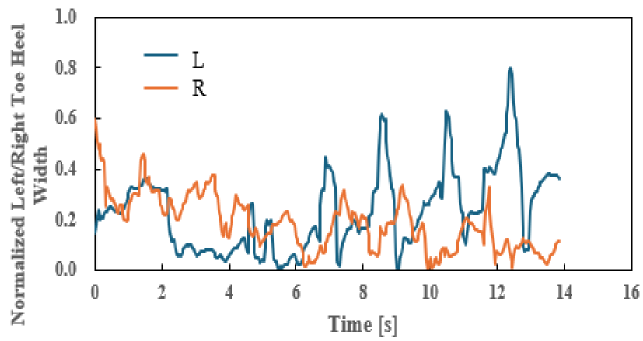

Figure 12. Normalized width between toes and heels of right and left feet 72 d after onset.

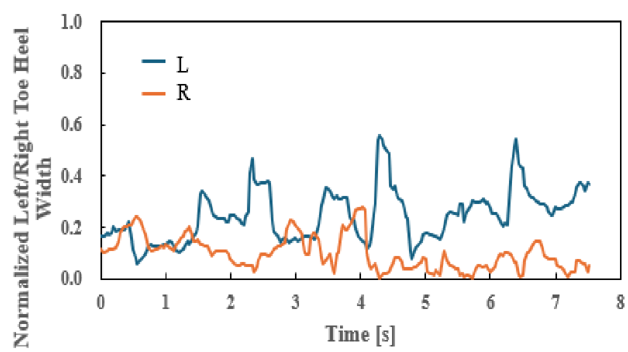

Figure 13. Normalized width between toes and heels of right and left feet 109 d after onset.

E. *Blurring between left and right elbow widths*

Figures 14 and 15 show the blurring between the left and right elbow widths 72 and 109 days after onset, respectively. As depicted, the width decreased at 109 d after the onset. The horizontal axis in Figures 14 and 15 shows the time in seconds, and the vertical axis shows the left and right elbow widths normalized by the waist width.

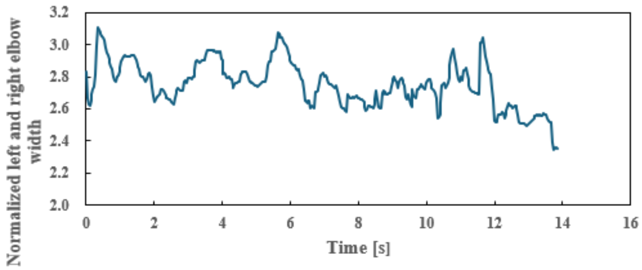

Figure 14. Normalized left and right elbow widths 72 d after onset.

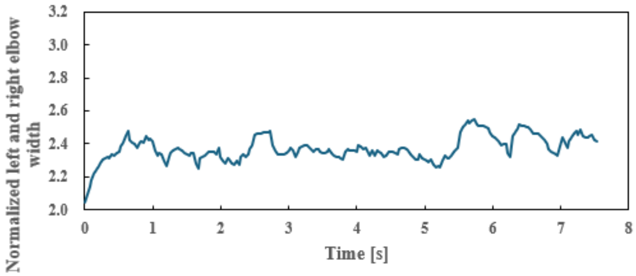

Figure 15. Normalized left and right elbow widths 109 d after onset.

Figures 16 and 17 show the blurring between the left and right elbow widths normalized by the shoulder width 72 and 109 d after onset, respectively. As depicted, the width decreased at 109 d after the onset. The horizontal axis in Figures 16 and 17 shows the time in seconds, and the vertical axis shows the shoulder width normalized by the widths of the left and right elbows.

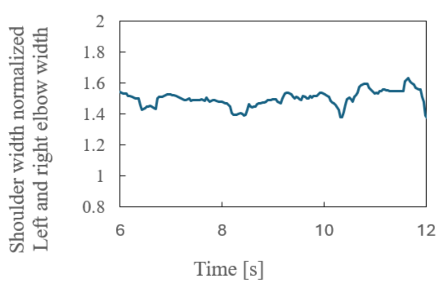

Figure 16. Normalized left and right elbow widths 72 d after onset.

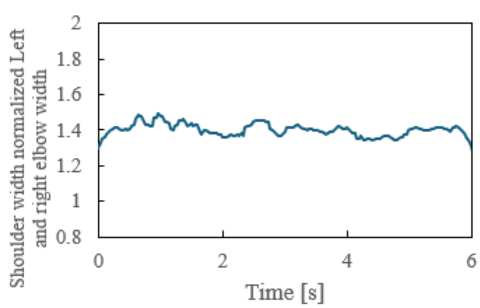

Figure 17. Shoulder-normalized left and right elbow widths 109 d after onset.

F. Temporal changes in knee and ankle during gait

Figures 18 and 19 show the left and right knee and ankle heights at 72 and 109 days after onset, respectively, normalized by the waist width. In Figures 18–20, the horizontal axis shows the time, in seconds, and the vertical axis shows the knee and ankle from the normalized waist.

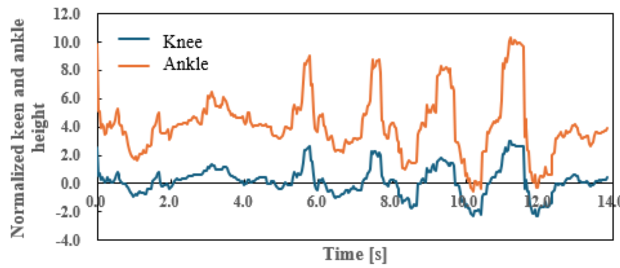

Figure 18. Normalized left knee and left ankle heights 72 d after onset.

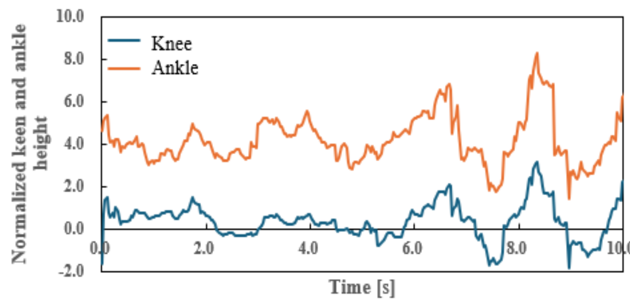

Figure 19. Normalized right knee and right ankle heights109 d after onset.

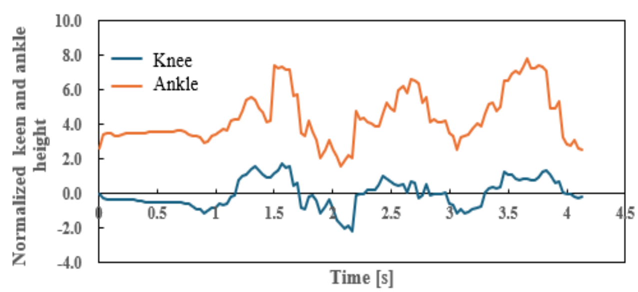

Figure 20. Left knee and ankle heights of Participant D.

Figure 20 shows the left knee and ankle heights normalized by the width of Participant D's waist as a reference.

G. Example of stride length

Figures 21 and 22 show the left and right heel heights of Participant B during walking, respectively, normalized by the hip width. They were measured 18 d after symptom onset. In these figures, the inclination was corrected based on distance. Stride length is defined as the distance from the minimum value to the next minimum value. The area indicated by a square in the figure represents the stride length. At approximately 5, 12, and 17 s, for the left ankle shown in the figure, the maximum value was followed by the minimum value, and data that could not be considered as one step were obtained. However, by comparing the data for the right ankle and watching the video, we confirmed that the ankle was not stepping forward owing to greater unsteadiness. Therefore, a wider width was not considered as one step. The horizontal axis in Figures 21–24 shows the time in seconds, and the vertical axis shows the relative position of the ankle with correction.

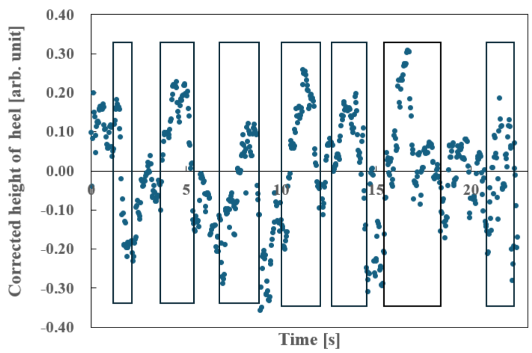

Figure 21. Left-heel height during walking of Participant B normalized by hip width.

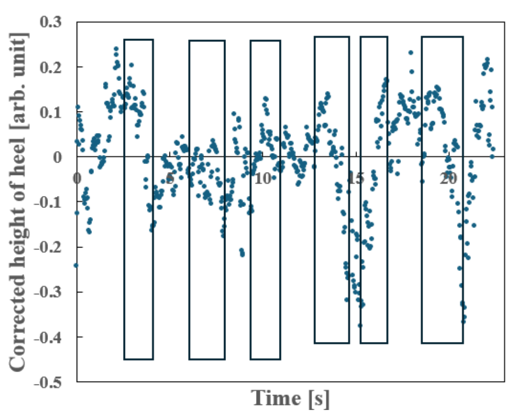

Figure 22. Right-heel height during walking of Participant B normalized by hip width.

Figures 23 and 24 show the left and right heel heights of Participant C during walking, respectively, normalized by the hip width. They were measured 18 d after symptom onset. In these figures, the inclination was similarly corrected based on the distance. Stride length is defined as the distance from the minimum value to the next minimum value. The area indicated by a square in the figure represents the stride length. At approximately 5 s, for the left ankle shown in the figure, the maximum value was followed by the minimum value, and data that could be considered as one step were obtained. However, by comparing the data for the right ankle and watching the video, we confirmed that the ankle was not stepping forward owing to greater unsteadiness. Therefore, a wider width was considered as one step.

Additionally, we viewed the video to determine whether the data for the right foot at 11 and 15–17 s varied. We discovered that the ankle was unsteady and thus could not to identify a clear step; therefore, we excluded it from the calculations of stride length and speed.

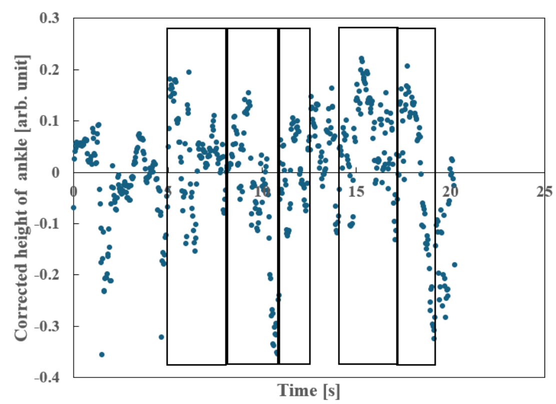

Figure 23. Left-heel height during walking of Participant C normalized by hip width.

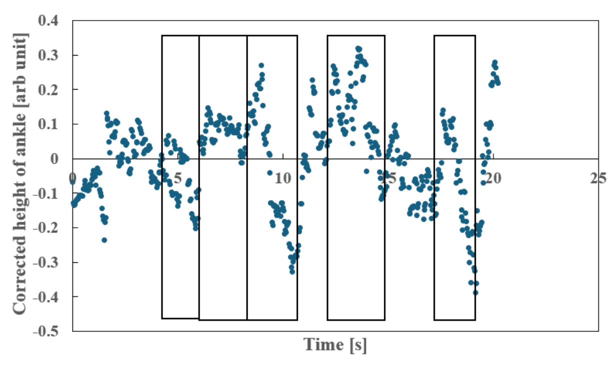

Figure 24. Right-heel height of Participant C during walking normalized by hip width.

The first and second measurements of stride length and foot speed for the three participants (A–C) are listed in Tables 4 and 5. These ratios are listed in Table 6.

Table 4. Step length and speed results for first measurement.

	Left stride length [cm]	Right stride length [cm]	Left foot speed [cm/s]	Right foot speed [cm/s]
Participant A	55.2	83.2	31.8	49.5
Participant B	36.1	35.8	8.7	8.5
Participant C	36.1	35.3	8.8	8.5

Table 5. Step length and speed results for second measurement.

	Left stride length [cm]	Right stride length [cm]	Left foot speed [cm/s]	Right foot speed [cm/s]
Participant A	116.0	83.3	78.3	49.5
Participant B	27.9	28.7	16.3	15.1
Participant C	15.5	16.4	6.5	6.4

Table 6. Ratio of first and second measurements.

	Left stride length ratio	Right stride length ratio	Left foot speed ratio	Right foot speed ratio
Participant A	2.1	1.0	2.5	1.0
Participant B	0.8	0.8	1.9	1.8
Participant C	1.0	0.9	1.0	0.7

H. *Smart-insole pressure sensor*

For Participant B, we obtained the insole-sensor data during the second walk; Figures 25 and 26 show the results for the left and right foot, respectively. The horizontal axis in Figures 25 and 26 shows the time in seconds, and the vertical axis shows the relative value output from the insole sensor.

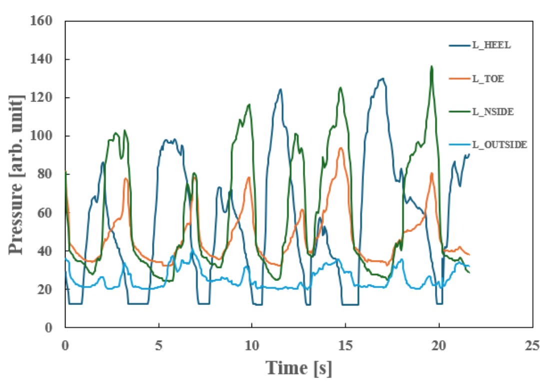

Figure 25. Pressure on four parts of left foot.

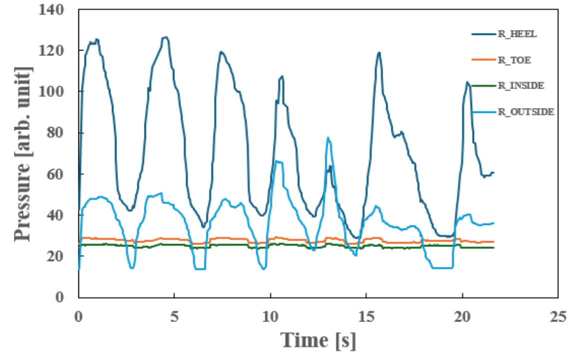

Figure 26. Pressure on four parts of right foot.

The pressure on the outside of the left foot was low. Pressure was applied sequentially from the heel to the inside of the foot and to the toes. However, for the right foot, a high pressure was applied simultaneously to the heel and outside. The pressures on the toes and inside the foot were low, although they were applied at almost the same time.

I. *Spectrogram*

In Figures 27–29, the horizontal axis represents time in seconds, and the vertical axis represents frequency, with different colors indicating the output intensity. The spectral variation over time was calculated via the discrete Fourier transform at every second. The horizontal axis represents the time; the vertical axis represents the frequency; and the spectral intensity (square root of the power spectrum) is shown in red, yellow, green, blue, and black. A rectangular window is used as the time-window function.

The spectrograms of the left and right ankles of Participant A are shown in Figure 27. Owing to the improved foot speed, the second measurement spanned the same distance as the first measurement in approximately 7 s; therefore, the display time was shorter. In Figure 27, (a1) and (a2) show the first and second measurement results for the left ankle, respectively; and (b1) and (b2) show the first and second measurements for the right ankle, respectively.

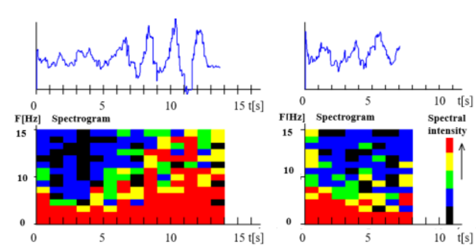

(a1) (a2)

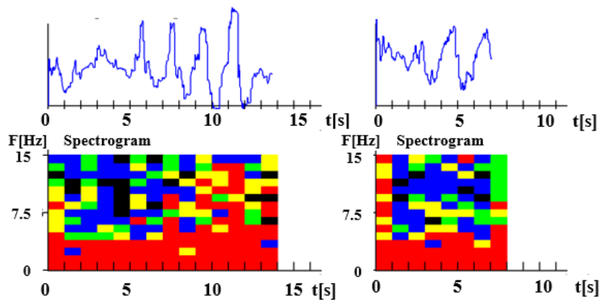

Figure 27. Spectrograms of left and right ankles of Participant A.

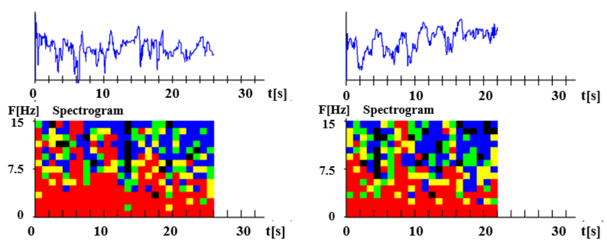

(a1) (a2)

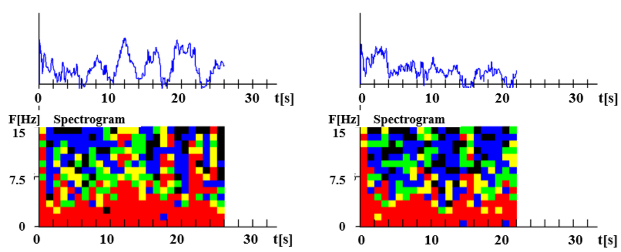

(b1) (b2)

Figure 28. Spectrograms of left and right ankles of Participant B.

The spectrograms of the left and right ankles of Participant C are shown in Figure 29. The second measurement for Participant C was performed approximately one month after rehabilitation. The video showed that compared with the other participants, Participant C received less assistance from the caregiver and was walking carefully while observing his feet, which reduced his foot speed. This resulted in a longer measurement time.

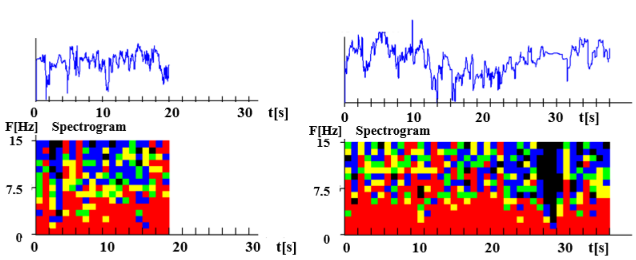

(a1) (a2)

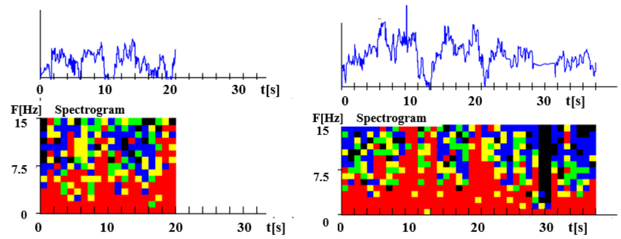

(b1) (b2)

Figure 29. Spectrograms of left and right ankles of Participant C.

IV. DISCUSSION

The authors acknowledge that this study included only three rehabilitated participants (A–C) and one healthy participant. Thus, a cohort study with more participants may be necessary for a more detailed analysis.

We will separately examine the extent to which the differences can be detected between the first and second measurements of the participants using MediaPipe's skeletal recognition data, which were obtained from videos captured from the anterior frontal direction.

A. Difference in normalized left and right ankle heights due to hip width

Normalization by the hip width allowed us to obtain the amplitude of the foot height (even in the early phase) away from the camera, based on which a flat area was observed. This information can be used to determine the stance and swing phases, although a detailed study has not yet been conducted.

B. Normalized shoulder angle

The first-order component was not in the exact frontal direction at the time of the video recording. This might be because the gait began slightly to the left of the center of the screen and eventually shifted to the right. The linear component can be attributed to the gait commencing slightly to the left of the center of the screen and eventually shifting to the right.

C. Blurring of nose position

A previous study showed that using an attachment with an assist function improved leg swing and reduced nose wobble. Therefore, we used the data in the two tables 1 and 2 to examine whether this idea is applicable for improving rehabilitation.

When Participant A's variance of the horizontal value in the travel direction was used to blur the nose position, the blurring width increased slightly, and the variance values were 1.6×10^{-4} and 2.7×10^{-4}. However, based on the data in Tables 3 and 5, we can conclude that the shift in weight from left to right became more balanced and the foot speed improved, owing to an increase in the foot speed 109 d after symptom onset. Therefore, by comparing the left and right deviations of the nose, we can determine whether the weight can be shifted sideways. Considering this value and the deviation in the ankle height, we can evaluate whether the participant was walking in a well-balanced manner.

Considering these two points, which show that Participant A's relative nose position deviation was 1.3 times larger after 109 d and that the speed of the left leg swing increased, as shown in Table 5, we can conclude that Participant A was now able to shift her weight more smoothly. As shown by the blurring of the nose position in Figures 6 and 7, the shift became a large left-right shift smoothly, which is an indicator of recovery. For Participants B and C, the left-right shift was less smooth than that for Participant A. However, this is regarded as an indicator of recovery in conjunction with the content in subsection G, which discusses the stride length and speed.

D. Change in width between toe and heel

In the early phase of rehabilitation, the toe and heel widths of the paralyzed left foot were large, which affected the widths of the right toe and heel. Additionally, 109 d after symptom onset, the left toes and heels became narrower and improved, which caused the right toes and heels to become smaller.

E. Blurring between left and right elbow widths

The elbow width during walking was reduced by approximately 20% between the pre-rehabilitation period and 109 d after symptom onset, thus confirming the beneficial effects of rehabilitation. Based on Figures 16 and 17, normalization by shoulder width was effective, as evidenced by the reduced blur width.

F. Temporal changes in knee and ankle during gait

The temporal difference between the knee and ankle was not evident in this experiment using MediaPipe, although the knee was slightly ahead of the ankle when evaluated on the time axis in some cases. By contrast, the analysis of the experiment conducted with Participant B did not reveal a time difference between the knee and ankle onset of movement.

G. Stride and gait speed

The following were concluded by comparing the left and right stride lengths and left and right foot-movement speeds between the first and second measurements of three participants (A, B, and C): Participant A, who showed recovery, had almost the same stride length and movement speed as the right foot, whereas the stride length and movement speed of the paralyzed left foot showed significant improvement.

Participant B's stride length changed marginally; however, his foot-movement speed increased, thus suggesting that the rehabilitation was effective.

No significant differences were observed in the calculation results for Participant C. Only slight difference was observed, which is attributable to differences in the degree of improvement among Participants A, B, and C and may reflect the degree of recovery.

Comparing the ratios of standard deviations, the standard deviations of the stride length and left-foot speed of Participants A and C decreased from 0.8 to 0.5 in the second measurement as compared with the first, which is considered an indicator of recovery. For Participant B, the ratio of standard deviations for both the stride length and gait speed increased by two to three times. This result, in combination with the insole-sensor results shown in Figures 26 and 27, indicates that the right leg shifted with the non-paralyzed left leg as the center of gravity, thus indicating the importance of using the results in combination with other assessments to evaluate recovery.

H. Smart-insole pressure sensors

Because the participant had right-sided paralysis, the left foot was subjected to pressure from the heel to the outer part and then to the toes. When the participant placed weight on the right foot, pressure was applied almost simultaneously, resulting in the flat-foot condition.

I. Spectrogram

The spectrogram of Participant A showed a significant improvement in the second measurement, although a fewer high-frequency components and a more stable walking pattern were observed.

In the second measurement shown in the spectrogram of Participant B, the paralyzed right leg showed a slight decrease in the number of high-frequency components. For the right leg, the number of high-frequency components decreased during walking, thus suggesting stable movement without blurring. This might reflect the difference in the manner by which weight was applied to the right foot, as shown by the results for the smart insole.

In the spectrogram of Participant C, even in the second measurement, the paralyzed right leg indicated a slight decrease in the number of high-frequency, thus suggesting the effectiveness of rehabilitation.

V. CONCLUSIONS

The effect of rehabilitation was verified using images captured from the frontal direction using MediaPipe. Standardization by hip width reduced the effect of the distance from the camera, and the change in gait was confirmed by determining the ankle height during walking, the tilt of the left and right shoulders, the width between the toes and heels, and the width between the left and right elbows. An evaluation method was demonstrated for cases in which images could not be captured easily from the sagittal plane and could only be captured from the frontal direction owing to limitations in imaging direction, which occurs in actual rehabilitation settings. Additionally, the effectiveness of shoulder normalization was demonstrated.

Walking ability and walking patterns are important for clinical gait assessment. Quantitative instrumental gait analysis is recommended for evaluating gait performance and quality in clinical settings; however, its current application remains insufficient. The results obtained in the current experiments were based on a short rehabilitation period and a small number of participants. To obtain more accurate conclusions, future studies should include a larger sample size and a long-term analysis.

Moreover, we cannot conclude that this assessment method is highly relevant for evaluating walking ability in real-life situations. Nevertheless, one patient demonstrated improvement in real-life walking ability.

ACKNOWLEDGMENT

This study was supported by the JSPS KAKENHI (grant numbers JP20K11924 and JP23K11207). We thank the patients and staff of the Isogo Central Hospital for their cooperation in this study.

REFERENCES

[1] Y. Uchida, T. Funayama, E. Ohkubo, D. Souma, and Y. Kogure, "Detecting Gait Changes with Front-Facing Video and MediaPipe: A Hemiplegic Patient Case Study," GLOBAL HEALTH 2024, pp. 10-15, IARIA, ISBN: 978-1-68558-189-3.

[2] A. A. Huueck, D. M. Mohan, N. Abdallah, M. E. Rich, and K. Khalaf, "Present and future of gait assessment in clinical practice: Towards the application of novel trends and technologies," Frontiers in Medical Technology, DOI 10.3389/fmedt.2022.901331, pp. 1-21, 2022.

[3] S. Campagnini et al, "Machine learning methods for functional recovery prediction and prognosis in post-stroke rehabilitation:a systematic review," Journal of NeuroEngineering and Rehabilitation," https://doi.org/10.1186/s12984-022-01032-4, pp. 1-22, 2022.

[4] V. Varma and M. Trkov, "Investigation of intersegmental coordination patterns in human walking," Gait & Posture, vol. 112, pp. 88-94, 2024.

[5] D. Xu et al., "A new method proposed for realizing human gait pattern recognition: Inspiration for the application of sports and clinical gait analysis," Gait & Posture, vol. 107, pp. 293-305, 2024.

[6] M. Windolf, N. Gotzen, and M. Morlock, "Systematic Accuracy and Precision analysis of Video motion Capturing Systems-Exemplified on The Vicon-460 system," Journal of Biomechanics, vol. 41, pp. 2776-2780, 2008.

[7] T. B. Rodrigues, D. P. Salgado, C. O. Cathain, N. O'Connor, and N. Murray, "Human Gait Assessment Using a 3D Marker-less Multimodal Motion Capture System," Multimedia Tools and Applications vol. 79, pp. 2629-2651, 2020.

[8] P. Plantard, E. Auvinet, A. S. Le Pierres, and F. Multon,"Pose Estimation with a Kinect for Ergonomic Stuidies: Evaluation of the Accuracy Using a Virtual Mannequin," Sensors, pp. 1785-1803, 2015.

[9] R. A. Clark, B. F. Mentiplay, E. Hough, and Y. H. Pus, "Three-Dimensional Cameras and Skeleton Pose Tracking for Physical Function Assessment: A Review of Use, Validity, Current Developments and Kinect Alternatives," Gait & Postture, vol. 68, pp. 193-200, 2019.

[10] J. A. Albert el al., "Evaluation of the Pose Tracking Performance of the Azure Kinect and Kinect v2 for Gait Analysis in Comparison with a Gold Standerd: A Pilot Study, Sensors, vol. 20, 5104, 2020.

[11] Y. Ma, K. Mithratatne, N. Wilson, Y. Zhang, and X. Wang, "Kinect v2-Based Gait Analysis for Children with Cerebral Palsy: Validity and Reliability of Spaial Margin of Stability ad Spationtemporal Vaiables," Sensors, vol. 21, 2104, 2021.

[12] D. Imoto, S. Hirano, M. Mukaino, E. Saitoh, and Y. Otaka, "A Novel Gait Analysis System for Detecting Abnormal Hemiparetic Gait Patterns during Robo-assisted Gait Training : A Criterion Validity Study among Healthy Adults," Frontiers in Neurorobotics, 16:1047376, 2022.

[13] G. Hidalgo et al., "CMU-Perceptual-Computing-Lab," Avairable: https://gitgub.com/CMU-Preceptual-Computing-Lab/openpose, retrieved: August, 2024.

[14] Z. Cao, G. Hidalgo, T. Simon, S-E. Wei, and Y. Sheikh, "OpenPose: Realtime Multi-Person 2D Pose Estimation Using Part Affinity Fields," IEEE Transaction on Patern Analysis and Machine Intelligence, vol. 43, pp. 172-186, 2021.

[15] N. Nakano et al., "Evaluation of #D Markerless Motion Capture Accuracy Using OpenPose With Multiple Video Cameras," Frontiers in Sport and Active Living, vol. 20, Article 50, 2020, doi:10.3389/fspor.2020.00050.

[16] M. Ota, H. Tateuchi, T. Hahiguti, and N. Ichihasi, "Verification of validity of gait analysis systems during treadmill walking and running using human pose tracking algorithm," Gait and Posture, vol. 85, pp. 290-297, 2021.

[17] Y. Saiki et al., "Reliability and validity of OpenPose for measuring hip knee ankle angle in patients with knee osteoarthritis," Scientific Reports, vol. 13, 3297, 2023.

[18] V. Bazarevsky et al., "BlazePose: On-device Real-time Body Pose tracking," arXiv:2006.1204v1 [cs.CV] 2020.

[19] G. Kaur, G. Jaju, D. Agawal, K. Lyer, and C. M. Prashanth, "Implementation of Geriatric Agility Detection Using MediaPipe Pose," International Journal of Recent Advances in Multidisciplinary Topics, vol. 3, 119, 2022, ISSN:2582-7839.

[20] Y. Uchida, T. Funayama, and Y. Kogure, "Investigation of the Application of MediaPipe to Gait Analysis," pp. 1-6, IARIA, 2022. ISBN: 978-1-61208-995-9.

[21] Y. Uchida, T. Funayama, and Y. Kogure, "Possibility of Gait Analysis with MediaPipe and Its Application in Evaluating the Effects of Gait-assist Devices," pp. 44-54, IARIA, International Journal on Advances in Life Sciences, vol. 15, no. 1 & 2, 2023.

[22] J.-L. Vhung, L.-Y. Ong, and M-C. Leow, "Comparative Analysis of Skelton-Based Human Pose Estimation," Future Internet, vol. 14, 380, 2022.

[23] Y. Uchida, T. Funayama, E. Ohkubo, and Y. Kogure, "Considerations for Applying MediaPipe to Gait Analysis," GLOBAL HEALTH 2023, pp. 12-17, IARIA.

[24] S. Kim et al., "Assessing physical abilities of sarcopenia patiens using gait analysis and smart insole for development of digital biomarker," Scientific Reports, vol. 13, 10602, 2023, https://doi.org/10.1038/s41598-023-37794-7.

[25] Y. Fan, "The Gesture Recognition Improvement of Mediapipe ModelBased on Histrical TrajectoryAssist Tracking Kalman Filtering and Smooth Filterling," CISAI 2024, Shaoxing, China, pp. 641-674.

[26] M. Lei, Z. Wang, and F. Chen, "Ballet Form Traning Based on MediaPipe Body Posture Monitoring," Journal of Physics: Conference Series, ICAITA-2023, 2637(2023)012019, doi:10.1088/1742-6596/2637/1/012019.

[27] D. Deng et al., "Interpretable video-based tracking and quantification of parkinsonism clinical motor stated," npj Parkinson's Disease, (2024) 10:122, https://doi.org/10.1038/s41531-024-00742-x.

[28] M. U. Friedrich et al., “Validation and application of computer visopn algorithms for video-based tremor analysis,” npj Digital medicine, (2024)7:165, https://doi.org/10.1038/s41746-024-01153-1.

[29] G. Colnella-Barba et al., “Using a Webcam to Assess Upper Extremity Proprioception: Extperrimental Validation and Application to Persons Post Stroke,” Sensors, vol.24, 7434, 2024.

[30] T. Funayama, Y. Uchida, Y. Kogure, D. Souma, and R. Kimura, “Exploring the Assessment of Steps Using Insoles with Four-Part Pressure Sensors,” Sensors & Transducers, vol. 263, pp. 21-28, 2023.